# Replacement of Connexin40 by Connexin45 in the Mouse
## Impact on Cardiac Electrical Conduction

Sébastien Alcoléa, Thérèse Jarry-Guichard, Jacques de Bakker, Daniel Gonzàlez, Wouter Lamers, Steven Coppen, Luis Barrio, Habo Jongsma, Daniel Gros, Harold van Rijen

***Abstract***—Gap junction channels, required for the propagation of cardiac impulse, are intercellular structures composed of connexins (Cx). Cx43, Cx40, and Cx45 are synthesized in the cardiomyocytes, and each of them has a unique cardiac expression pattern. Cx40 knock-in Cx45 mice were generated to explore the ability of Cx45 to replace Cx40, and to assess the functional equivalence of these two Cxs that are both expressed in the conduction system. ECGs revealed that the consequences resulting from the biallelic replacement of Cx40 by Cx45 were an increased duration of the P wave, and a prolonged and fractionated QRS complex. Epicardial mapping indicated that the conduction velocities (CV) in the right atrium and the ventricular myocardium, as well as conduction through the AV node, were unaffected. The significant reduction of the CV in the left atrium would be the most likely cause of the P-wave lengthening. In the right ventricle, a changed and prolonged activation in sinus rhythm was found in homozygous mutant mice, which may explain the prolongation and splitting of the QRS complex. Electrical mapping of the His bundle branches revealed that this was due to slow conduction measured in the right branch. The CV in the left branch was unchanged. Therefore, in the absence of Cx40, the upregulation of Cx45 in the heart results in a normal impulse propagation in the right atrium, the AV node, and the left His bundle branch only. **(*Circ Res*. 2004;94:100-109.)**

**Key Words:** gap junction channels ■ connexins ■ cardiac conduction

In the mammalian heart the electrical activity, spontaneously generated in the sinoatrial (SA) node, is propagated through the atria, then to the ventricular walls via specialized tissues that constitute the conduction system (CS). The CS includes the atrioventricular (AV) node, the His bundle, and the two bundle branches (BBs), which ramify into peripheral Purkinje fibers. Gap junction channels are responsible for the electrical coupling between the various types of myocytes, and they are required for the propagation of cardiac impulse.[1]

Gap junction channels are intercellular structures constituted by transmembrane proteins belonging to the connexin (Cx) family.[2,3] Nineteen Cx genes have been identified in the mouse genome,[4] but so far only four Cxs, Cx43, Cx40, Cx45, and Cx46, have been shown to be expressed in mammalian cardiomyocytes with each having a unique expression pattern in the adult heart.[5] Hence, in the mouse heart, Cx43 is abundant in both the atrial and ventricular working myocytes, and the distal part of the CS; Cx40 is strongly expressed in the atrial working myocytes and the CS,[6,7] whereas Cx45 is detected mainly in the SA node and the CS.[8–10] Expression of Cx45 has been reported in the working ventricular myocardium[11] but this finding has not been corroborated by other investigations.[9,12] Lastly, Cx46 was detected in the rabbit SA node associated with Cx40 and Cx45.[13,14]

Analysis of Cx-deficient mice has provided evidence that Cx43, Cx40, and Cx45 are involved in both heart function and development. The Cx45 null mutation is lethal with the embryos dying in utero around embryonic day 10, 2 days after cardiac contractions are normally initiated.[15,16] Several anomalies including defects in the endocardial cushions are thought to contribute to the lethal phenotype. Conditional knock-out (KO) mice in which Cx43 gene expression in the cardiomyocytes is reduced by about 90% have ventricular conduction velocity (CV) slowed by 50%. All these mice undergo sudden cardiac death from spontaneous ventricular arrhythmias by 2 months of age.[17] Cx40KO mice are viable and fertile,[18,19] and several studies have focused on impulse propagation in the hearts of these mice.[20–25] Findings from these studies include impaired conduction at various levels of the CS, and increased incidence of inducible atrial tachyarrhythmias, indicating that Cx40 is an important determinant of impulse propagation in the atria and the AV conduction system. Recent investigations also suggest that Cx40 may play a role in cardiac morphogenesis.[26]

Original received May 12, 2003; resubmission received October 2, 2003; revised resubmission received November 6, 2003; accepted November 11, 2003.

From the Laboratoire de Génétique et Physiologie du Développement (UMR CNRS 6545) (S.A., T.J.-G., D.G.), Institut de Biologie du Développement de Marseille, Université de la Méditerranée, Marseille, France; Department of Medical Physiology (H.v.R., H.J.), University Medical Center, Utrecht, The Netherlands; Neurologia Experimental (D.G., L.B.), Hospital Ramón y Cajal, Madrid, Spain; Interuniversity Cardiology Institute (J.d.B.), Utrecht, The Netherlands; Department of Anatomy and Embryology (W.L.), Academic Medical Center, University of Amsterdam, Amsterdam, The Netherlands, and National Heart and Lung Institute (S.C.), Imperial College London, UK.

Correspondence to Dr Daniel Gros, LGPD/IBDM, Campus de Luminy, Case 907, 13288 Marseille, France. E-mail gros@ibdm.univ-mrs.fr



***Circulation Research*** **is available at http://www.circresaha.org** **DOI: 10.1161/01.RES.0000108261.67979.2A**

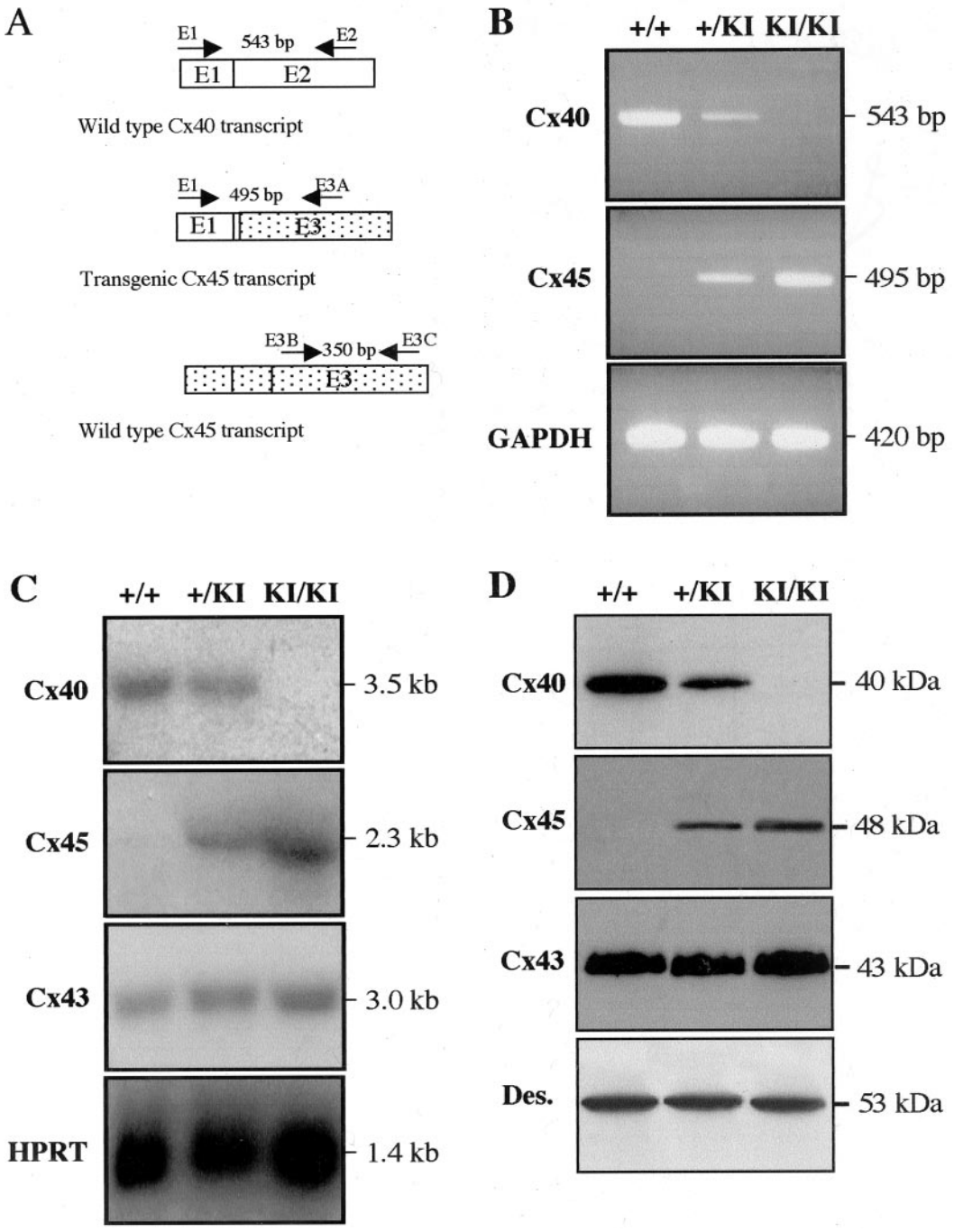


**Figure 1.** Expression of the transgene. A, Diagram indicating the positions of the primers (arrows) used in RT-PCR experiments to amplify fragments from wild-type (WT) Cx40, transgenic Cx45, and endogenous WT Cx45 transcripts. Transcribed exons 1 and 2 (E1 and E2) of the Cx40 gene are represented as white boxes. Transcribed exons 1, 2, and 3 of the Cx45 gene are represented as dotted boxes but only E3 is indicated. The expected sizes of amplicons are indicated. B, Representative results of RT-PCR experiments performed with RNA extracted from the atria of $Cx40^{+/+}$ (+/+), $Cx40^{+/KICx45}$ (+/KI), and $Cx40^{KICx45/KICx45}$ (KI/KI) 129Sv/CD1 mice. Similar results were obtained with 129Sv/C57Bl/6 mice. Amplicons of the expected sizes were detected in all samples investigated. The intensity of the glyceraldehyde-3-phosphate dehydrogenase (GAPDH) signals indicated that equivalent amounts of synthesized cDNAs were analyzed. C, Representative results of Northern blot experiments performed with RNA extracted from atria of $Cx40^{+/+}$ (+/+), $Cx40^{+/KICx45}$ (+/KI), and $Cx40^{KICx45/KICx45}$ (KI/KI) 129Sv/CD1 mice. Similar results were obtained with 129Sv/C57Bl/6 mice. Intensity of signals obtained with the hypoxanthine phosphoribosyl-transferase (HPRT) probe indicated that equal amounts of cDNA were analyzed. Exposure times: 3 days, 5 days, 1 day, and 12 hours after hybridization with Cx40, Cx45, Cx43, and HPRT probes, respectively. D, Representative results of Western blot experiments performed with samples of atrial tissue collected from $Cx40^{+/+}$ (+/+), $Cx40^{+/KICx45}$ (+/KI), and $Cx40^{KICx45/KICx45}$ (KI/KI) 129Sv/CD1 mice. Similar results were obtained with 129Sv/C57Bl/6 mice. Intensity of the signals obtained after treatment with anti-desmin antibody (Des.) indicated that similar amounts of proteins were probed with each of the anti-Cx antibodies. Molecular mass of the detected proteins is indicated on the right.

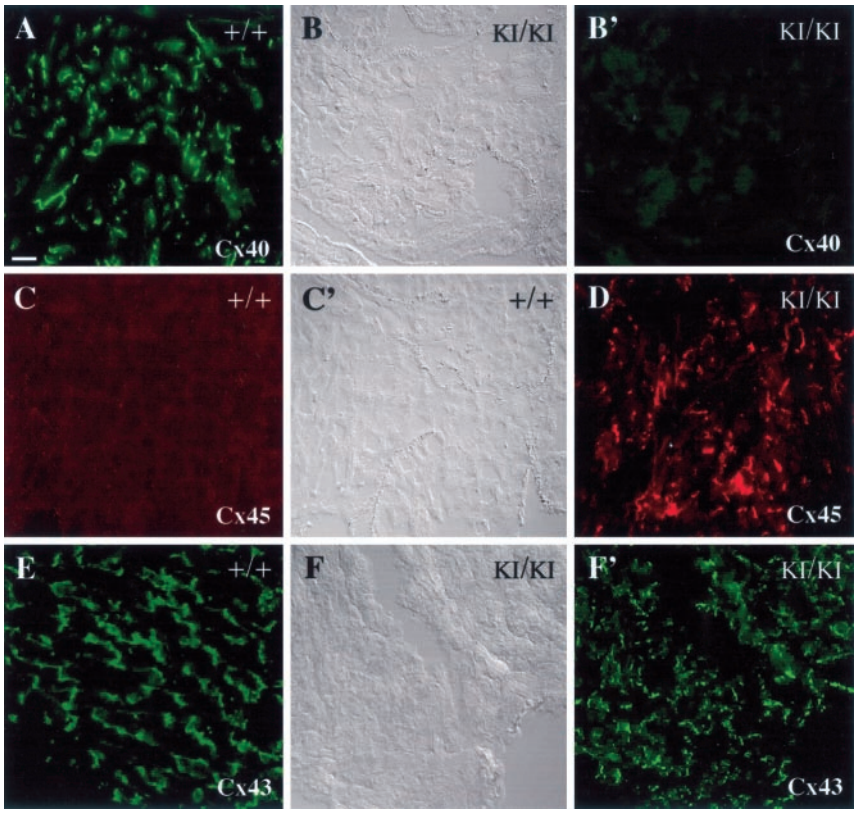


**Figure 2.** Expression pattern of Cxs associated with myocytes in the atria of WT and transgenic adult mice. Shown are micrographs of frozen sections from atria of $Cx40^{+/+}$ (+/+) and $Cx40^{KICx45/KICx45}$ 129Sv/C57Bl/6 mice (KI/KI). Sections were treated with rabbit anti-Cx40 (A and B'), anti-Cx45 (C and D), or anti-Cx43 (E and F') antibodies. A, B', C, D, E, and F', Immunofluorescence micrographs. B, C', and F are Nomarski micrographs of sections shown in B', C, and F', respectively. Similar results were obtained with 129Sv/CD1 mutant mice. Bar=20 $\mu$m for A through F'.

The analysis of KO mice has therefore provided important information on the in vivo functions of Cxs in heart. Another approach for analyzing the function of Cxs is to generate knock-in (KI) mice to assess the functional equivalence of two Cxs. Cx40 and Cx45 are both expressed in the mouse CS, albeit with very different levels of expression. Channels composed of Cx40 or Cx45 have quite different properties. Cx40 channels have a large unitary conductance (≈160 pS), in contrast with Cx45 channels, which have a small conductance (≈30 pS).[27,28] Macroscopic conductance of Cx40 channels is not very sensitive to the transjunctional voltage ($V_j$) as compared with that of Cx45 channels, which is very sensitive to $V_j$.[29–32] Furthermore, both types of channels are differently regulated by phosphorylation.[28,33] To assess the functional equivalence of Cx40 and Cx45, we have generated Cx40KICx45 mouse lines in which Cx45 is expressed in lieu and place of Cx40.

## Materials and Methods

The strategy used to generate the transgenic mice and the techniques used for genotyping the ES cells and mice and for identifying expression of the transgene in the KI mice are described in detail in the expanded Materials and Methods in the online data supplement (available at http://www.circresaha.org). The expression of the transgene was assessed on three hearts from adult mice (8 to 12 weeks old), from three independent litters, for each type of experiment carried out (RT-PCR, Northern and Western blots, immunofluorescence), and for each genotype investigated. In addition, all experiments were performed with samples from both Sv129/CD1 and 129Sv/C57Bl/6 mice.

ECG recordings were performed on anesthetized mice as described previously.[25,34] The hearts were dissected, connected to a Langendorff setup, and extracellular epicardial electrograms were recorded during sinus (SR) or paced rhythm.[25,34] Protocols for measuring epicardial activation and the conduction velocity (CV) in the various cardiac tissues including the BBs are described in the online data supplement. Multiple group comparisons were performed using ANOVA with LSD post hoc analysis using SPSS 10 for Macintosh. Values are mean±SEM. Values of $P \leq 0.05$ were considered statistically significant.

## Results

### Generation of the KI Mice

KI mice were generated on two genetic backgrounds:129129/CD1 (50%/50%) and 129Sv/C57Bl/6 (50%/50%). No abnormal embryonic lethality was detected. The mice grew normally, were fertile, and had no obvious anatomical cardiac defects.

### Transcriptional and Translational Expressions of the Transgene

The results revealed no significant difference dependent on the genetic background and were reproducible for each type of experiment performed.

The expression of Cx40, Cx43, and transgenic Cx45 mRNAs in the atria of wild-type (wt, $Cx40^{+/+}$), heterozygous ($Cx40^{+/KICx45}$) and homozygous ($Cx40^{KICx45/KICx45}$) mice was determined by semiquantitative RT-PCR (Figure 1B) and Northern blot experiments (Figure 1C). No endogenous Cx45 expression was detected (Figures 1B and 1C), but a gene-dependent gain of Cx45 mRNA, accompanied by a gene-dependent loss of Cx40 transcript (Figures 1B and 1C) was seen in $Cx40^{+/KICx45}$ and $Cx40^{KICx45/KICx45}$ mice. The expression level of Cx45 mRNA in $Cx40^{KICx45/KICx45}$ mice was comparable to that of Cx40 mRNA in $Cx40^{+/+}$ mice (Figures 1B and 1C).

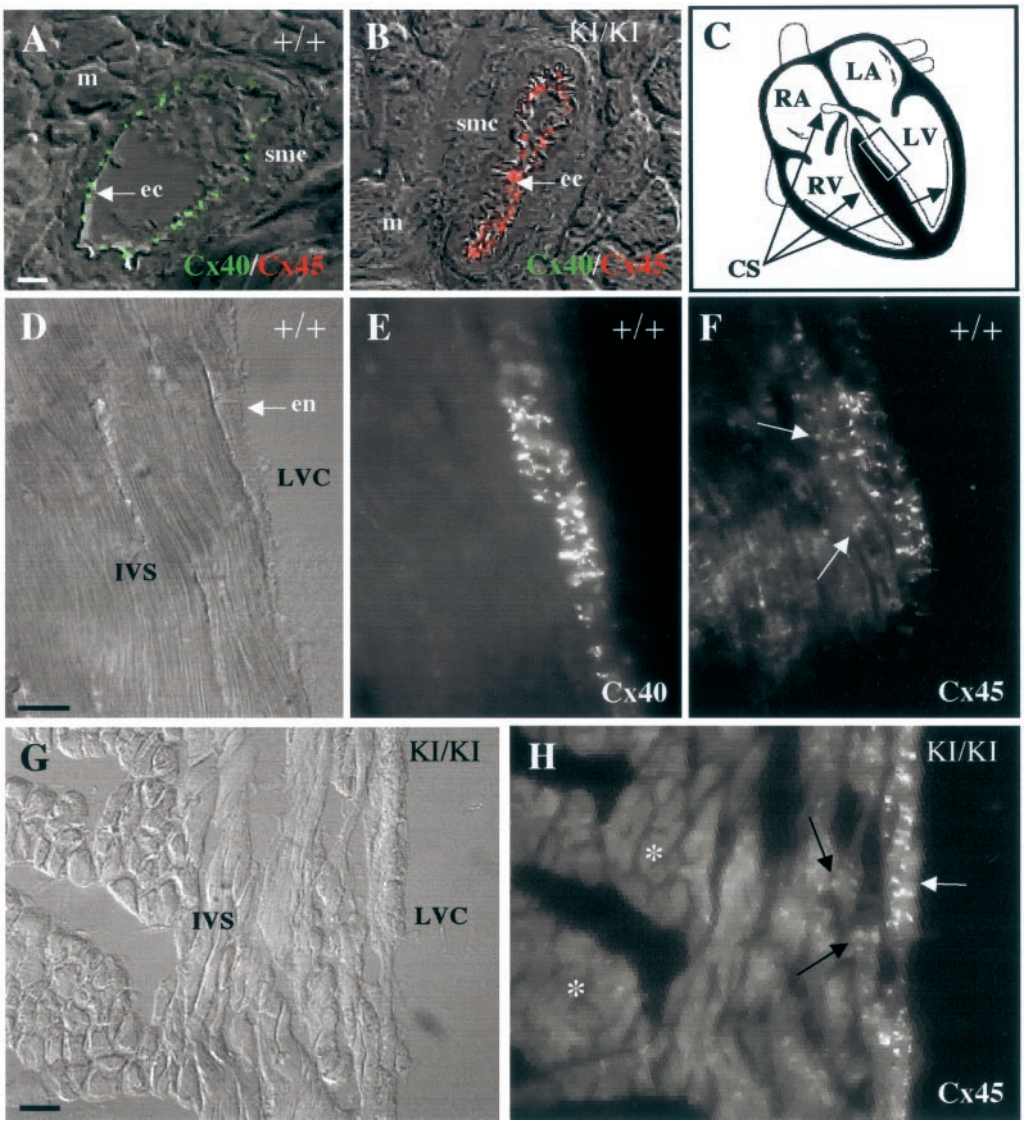


**Figure 3.** Expression pattern of Cxs associated with myocytes in the ventricles of WT and transgenic adult mice. Shown are micrographs of frozen sections from the ventricles of $Cx40^{+/+}$ (+/+) (A, D, E, and F) and $Cx40^{KICx45/KICx45}$ 129Sv/CD1 mice (KI/KI) (B, G, and H). Sections were treated with both rabbit anti-Cx40 antibodies (Cx40), and guinea pig anti-Cx45 antibodies (Cx45) (double-immunofluorescence technique). Superimposed Nomarski and immunofluorescence micrographs of sections of coronary vessels in the cardiac wall are presented in A and B. ec indicates endothelial cells; sm, smooth muscle cells; and m, myocytes. Cx40 detected between the endothelial cells of coronaries of $Cx40^{+/+}$ mice (A, green signals) has been replaced by Cx45 in $Cx40^{KICx45/KICx45}$ mice (B, red signals). D and G are Nomarski micrographs. en indicates endocardium; IVS, interventricular septum; and LVC, left ventricular chamber. E, F, and H are immunofluorescence micrographs. Position of the sections shown in these panels is indicated by a box in scheme C, which represents a mammalian heart. E and F, Subendocardial expression of Cx40 and Cx45, respectively, in a section (D) coming from the heart of a $Cx40^{+/+}$ mouse. Expression of both Cxs overlaps in the His bundle branch, but weak Cx45 labeling is also observed in the vicinity of the bundle, in the IVS (arrows in F). In the $Cx40^{KICx45/KICx45}$ mice (G and H), as in the $Cx40^{+/+}$mice, Cx45 was detected in the His bundle branches (white arrow in H), and in the first layer cells of the septal working myocytes (black arrows in H). It was undetectable in the major portion of the septum (asterisks in H). Similar results were obtained with 129Sv/C57Bl/6 mutant mice. Bar in A=50 $\mu$m for A and B; bar in D=50 $\mu$m for D, E, and F; and bar in G=20 $\mu$m for G and H.

The levels of expression of the transcript of the Cx43 gene in the three types of mice investigated were similar (Figure 1C).

Cx45 protein[12] was correctly translated in the transgenic mice, as shown by Western blot experiments performed with atrial samples (Figure 1D). The reduction of the level of expression of Cx40 protein in the atria of $Cx40^{+/KICx45}$ mice (Figure 1D) was associated with the detection of Cx45 protein in the same tissue. Cx40 protein was not detected in the atria samples of $Cx40^{KICx45/KICx45}$ mice. In contrast, Cx45 protein was shown to be expressed in these same samples with a level of expression higher than that observed in the heterozygotes. The level of expression of Cx43 protein was unaffected by the expression of the transgene (Figure 1D).

The pattern of expression of Cx40, Cx45, and Cx43 was further investigated by immunofluorescence on sections of $Cx40^{+/+}$ and $Cx40^{KICx45/KICx45}$ mouse heart. No signal was detected in the atria of $Cx40^{KICx45/KICx45}$ mice treated with anti-Cx40 antibodies (Figure 2B'), or in the atria of $Cx40^{+/+}$ mice treated with anti-Cx45 antibodies (Figure 2C). In contrast, analysis of sections from atria of $Cx40^{KICx45/KICx45}$

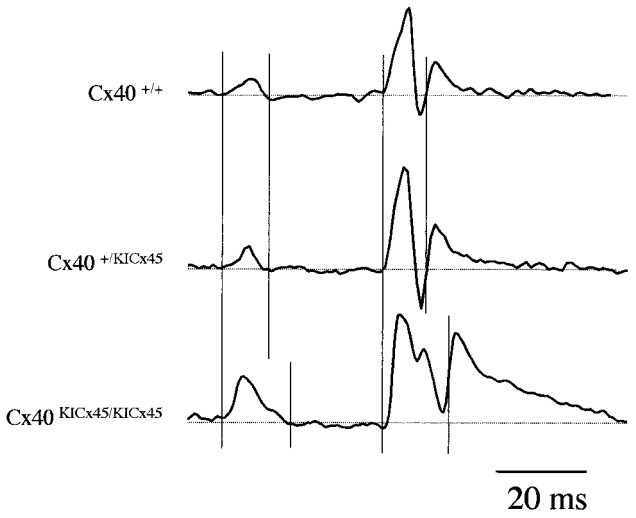


**Figure 4.** Representative ECGs recorded from $Cx40^{+/+}$, $Cx40^{+/KICx45}$, and $Cx40^{KICx45/KICx45}$ mice. Genetic background, 129Sv/CD1. Prolongation and fractionation of the QRS complex was observed in the $Cx40^{KICx45/KICx45}$ mice. Dotted lines represent isoelectric lines.

mice indicated that Cx45 was strongly expressed in this tissue with a pattern of expression similar to that of Cx40 in the samples of $Cx40^{+/+}$ mice (compare Figures 2A and 2D). The pattern of expression of Cx43, and the intensity of signals, were similar in the atria of both $Cx40^{+/+}$ and $Cx40^{KICx45/KICx45}$ mice (Figures 2E and 2F). Cx40 and Cx45 proteins were detected in the cardiac CS of $Cx40^{+/+}$ mice (Figures 3E and 3F), as reported previously.[5] The area of Cx45 labeling was larger than that of Cx40, corresponding to the so-called "extended conduction system,"[9] and the intensity of signal was weaker than that detected for Cx40 protein (Figures 3E and 3F). In the $Cx40^{KICx45/KICx45}$ mice the pattern of expression of Cx45 delineated an extended CS similar to that seen in the $Cx40^{+/+}$ mice (Figure 3H). Cx40 was detected between the endothelial cells of the coronaries irrigating the cardiac walls of the $Cx40^{+/+}$ mice (Figure 3A). In the coronaries of $Cx40^{KICx45/KICx45}$ mice, Cx45 had replaced Cx40, as expected (Figure 3B).

## Analysis of the Impulse Conduction in the Heart

### *Surface ECGs*

Figure 4 illustrates the ECG recordings of the 129Sv/CD1 mice. The values of the parameters of ECGs and their statistical analysis are summarized in the Table. No difference was found between the three genotypes investigated for the RR or the PQ intervals. However, the P wave duration was significantly increased from $9.1\pm0.3$ ms in the $Cx40^{+/+}$ mice to $10.7\pm0.5$ ms in the $Cx40^{KICx45/KICx45}$ mice, suggesting slower atrial activation or other mechanisms such as a delayed activation in the interatrial pathways or ectopic activation. The latter hypothesis is unlikely because the P-wave morphology was similar for all three genotypes. The QRS complexes were fractionated and their duration was increased from $10.8\pm0.4$ ms in the $Cx40^{+/+}$ mice to $14.0\pm0.6$ ms in the $Cx40^{KICx45/KICx45}$ mice, pointing to a delayed activation of the ventricles. The profiles of the ECGs of 129Sv/C57Bl/6 mice were similar to those of the 129Sv/CD1 mice (not shown). However the absolute values of the measured parameters were different from those of 129Sv/CD1 mice (Table), indicating a strain dependency, as expected.[35] The P wave and the QRS complex durations were significantly increased in the $Cx40^{KICx45/KICx45}$ 129Sv/C57Bl/6 mice, as compared with the $Cx40^{+/+}$ mice. Because the modifications identified were similar in the two genetic backgrounds, the experiments that followed were performed on one background only, 129Sv/CD1.

### *Ventricular Activation*

Epicardial mapping was performed in SR on Langendorff-perfused hearts to investigate the delayed activation of the ventricles in $Cx40^{KICx45/KICx45}$ mice. Figure 5 shows representative activation maps of the right (Figure 5A) and left ventricles (Figure 5B) in SR. In the $Cx40^{+/+}$ and $Cx40^{+/KICx45}$ mice, the sites of first activation were found as breakthrough, apicolateral, or basolateral sites (see Table for the frequencies of events). In the $Cx40^{KICx45/KICx45}$ mice no midventricular breakthrough activation was found, and the earliest activations were predominantly found at apical sites (Table), indicating a different mode of ventricular activation in these animals.

The total activation time was calculated from all RV and LV activation maps recorded in SR by subtracting the latest activation times from the earliest ones. The activation time of the RV was significantly increased from $5.4\pm0.4$ ms in $Cx40^{+/+}$ mice to $9\pm0.7$ ms (67%) in $Cx40^{KICx45/KICx45}$ mice (Table). The activation times of the LV of the mice of the three genotypes investigated were not significantly different (Table).

### *Atrioventricular Conduction*

Figure 5C shows examples of the AV delay as a function of the coupling interval of the premature stimulus (conduction curves). No significant differences were detected between the three groups of mice for neither the AV effective refractory period (ERP), the minimum AV delay at infinitely long coupling intervals ($D^{\infty}$), nor the time constant ($\tau$) (Table).

### *Atrial Conduction*

Activation maps of the paced right (RA) and left (LA) atria of the three groups of mice investigated are shown in Figures 6A and 6B, respectively. In the RA, the CV was $30.8\pm1.8$ cm/s for the $Cx40^{+/+}$ mice and was not significantly changed in the $Cx40^{+/KICx45}$ and $Cx40^{KICx45/KICx45}$ mice ($32.9\pm2.3$ and $30.0\pm2.3$ cm/s, respectively) (Table). In the LA, there was a significant reduction of the CV, from $31.5\pm1.6$ cm/s in $Cx40^{+/+}$ mice to $24.3\pm2.2$ cm/s in $Cx40^{KICx45/KICx45}$ mice.

### *Ventricular Conduction*

Examples of activation maps of the paced RV and LV are shown in Figures 6C and 6D, respectively. RV and LV activation maps showed anisotropic conduction independent of the genotype. Both longitudinal and transversal CVs in the ventricles were similar in all three genotypes (Table).

### *Bundle Branch Conduction*

Examples of RBB and LBB activation maps are shown in Figures 6E and 6F, respectively. RBB activation was always

**Electrophysiological Parameters of Wild-Type and Mutant Mice**

| | $Cx40^{+/+}$ | $Cx40^{+/KICx45}$ | $Cx40^{KICx45/KICx45}$ | ANOVA |
|---|---|---|---|---|
| ECG parameters, ms (129Sv/CD1) | | | | |
| RR interval | 126.5±11 (n=6) | 122.5±8.1 (n=11) | 120±5.6 (n=10) | 0.87 |
| P wave | 9.1±0.33 (n=6) | 9.3±0.4 (n=11) | 10.7±0.5 (n=10)*† | 0.034 |
| PQ interval | 34.8±0.7 (n=6) | 34.8±0.7 (n=11) | 35.8±1.1 (n=10) | 0.63 |
| QRS duration | 10.8±0.4 (n=6) | 10.5±0.3 (n=11) | 14±0.6 (n=10)*† | 0.001 |
| ECG parameters, ms (129Sv/C57Bl/6) | | | | |
| RR interval | 104.3±5.6 (n=14) | 103.9±3.3 (n=12) | 115±8.2 (n=13) | 0.36 |
| P wave | 9.4±0.31 (n=14) | 10.5±0.2 (n=12) | 12.2±0.5 (n=13)*† | 0.001 |
| PQ interval | 37±1.4 (n=14) | 36.4±0.9 (n=12) | 40.1±1.9 (n=13) | 0.19 |
| QRS duration | 10.2±0.2 (n=14) | 10.5±0.3 (n=12) | 12.5±0.5 (n=13)*† | 0.001 |
| Ventricular activation (129Sv/CD1) | | | | |
| Breakthrough RV (LV) | 33% (33%) | 11% (25%) | 0% (0%) | |
| Apical/lateral RV (LV) | 50% (50%) | 89% (37.5%) | 64% (92%) | |
| Basal/lateral RV (LV) | 17% (17%) | 0% (37.5%) | 36% (8%) | |
| RV activation time, ms | 5.4±0.4 (n=6) | 6.4±0.8 (n=9) | 9±0.7 (n=11)*† | 0.04 |
| LV activation time, ms | 6.1±0.8 (n=6) | 5.7±0.7 (n=8) | 6.7±0.5 (n=12) | 0.51 |
| Conduction velocities, cm/s (129Sv/CD1) | | | | |
| RA CV | 30.8±1.8 (n=6) | 32.9±2.3 (n=11) | 30.0±2.3 (n=12) | 0.63 |
| LA CV | 31.5±1.6 (n=6) | 35.6±3.1 (n=11) | 24.3±2.2 (n=11)*† | 0.01 |
| RV CV longitudinal | 37.5±2.7 (n=6) | 33.1±6.7 (n=10) | 33.8±2.2 (n=10) | 0.45 |
| RV CV transversal | 21.0±3.4 (n=6) | 21.2±2.0 (n=10) | 19.6±0.6 (n=10) | 0.80 |
| RV anisotropic ratio | 2.0±0.3 | 1.7±0.2 | 1.7±0.1 | 0.52 |
| LV CV longitudinal | 46.3±4.2 (n=6) | 39.1±3.2 (n=9) | 38.8±3.2 (n=12) | 0.33 |
| LV CV transversal | 20.5±1.1 (n=6) | 18.6±1.1 (n=9) | 16.1±1.0 (n=12) | 0.11 |
| LV anisotropic ratio | 2.3±0.3 | 2.2±0.2 | 2.3±0.2 | 0.8 |
| RBB CV | 36.5±5.4 (n=5) | 44.6±5.6 (n=9) | 19.2±2.9 (n=10)*† | 0.001 |
| LBB CV | 47.8±7 (n=5) | 49.2±3.5 (n=6) | 48±5.8 (n=6) | 0.98 |
| AV node function (129Sv/CD1) | | | | |
| AV ERP, ms | 68.3±4 (n=6) | 68±5.5 (n=10) | 74.2±5.1 (n=12) | 0.63 |
| AV delay t=∞, ms | 55.7±2.5 (n=6) | 64.2±3.5 (n=10) | 64.9±2.4 (n=12) | 0.12 |
| AV $\tau$ | 31.5±5.7 (n=6) | 22.13±1.8 (n=10) | 24.4±2.4 (n=12) | 0.14 |

Values are given as mean±SEM. *$P \leq 0.05$ compared to $Cx40^{+/+}$; †$P \leq 0.05$ compared to $Cx40^{+/KICx45}$. n indicates number of independent experiments.

recorded in a one-electrode wide strand, whereas LBB activation was electrically much wider and was always recorded in several electrode strands parallel to each other. In the $Cx40^{+/+}$ mice, the CV in the RBB was 36.5±5.4 cm/s (Table), and it was not significantly different in the $Cx40^{+/KICx45}$ mice. Interestingly, in the $Cx40^{KICx45/KICx45}$ mice, the CV in the RBB was significantly reduced by 46% to 19.2±2.9 ms. The CVs in the LBB were not significantly different between the three genotypes investigated (Table).

## Discussion

The targeted replacement of one Cx gene by another Cx gene has been performed for several Cxs.[36–38] Analysis of the resulting transgenic mice has indicated that Cxs could have either unique or redundant functions, and has provided important clues regarding the role of Cxs in vivo. In this study, we have generated Cx40KICx45 mice, and assessed the involvement of Cx45 in the propagation of cardiac impulse in the absence of Cx40.

For both genetic backgrounds investigated, the major phenotypic effects of the biallelic replacement of Cx40 by Cx45 were an increased duration of the P wave, and a prolonged and fractionated QRS complex in the ECGs in vivo. Epicardial mapping indicated a changed and prolonged activation of the RV that could be attributed to slow conduction in the RBB. The CVs in ventricular working myocardium, and the conduction delay in the AV node, were unaffected. The duration of the P wave was increased by about 18% in the $Cx40^{KICx45/KICx45}$ mice. No decrease of the CV in the RA was found in contrast to the LA in which a significant reduction of about 23% was observed. These data may explain the increase of the P-wave duration, although a delayed activation between the right and left atrium cannot be excluded, and indicate that Cx45 cannot fully replace the function of Cx40, at least in the LA. Studies on Cx40 KO

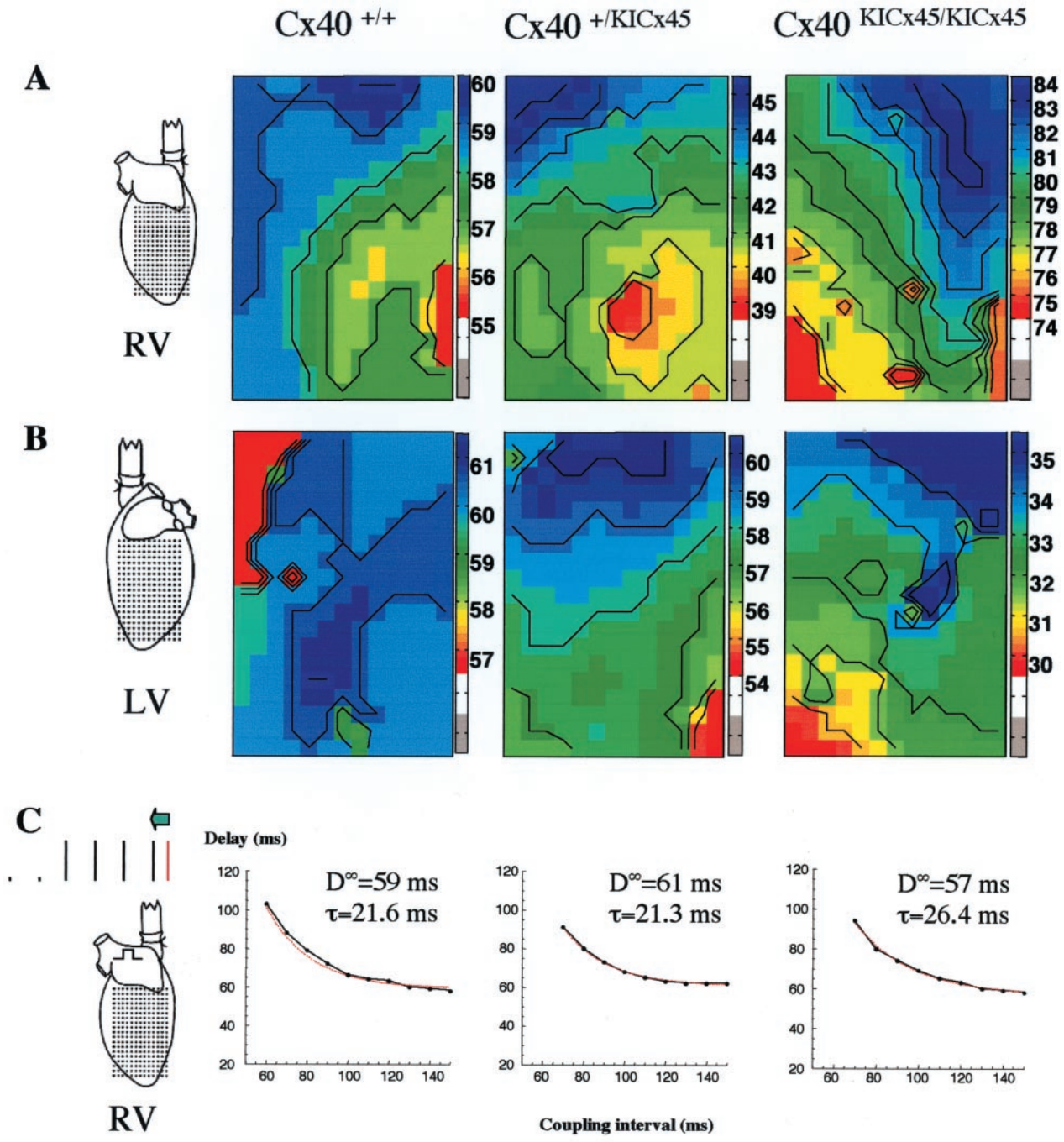


**Figure 5.** A and B, Representative examples of epicardial activation of the RV (A) and the LV (B) recorded in SR. Position of the electrode array on the epicardium is indicated in the pictograms. Activation times (ms) are indicated in A and B by color codes. In the maps shown in A, the sites of first activation were apicolateral, breakthrough, and basolateral sites for $Cx40^{+/+}$, $Cx40^{+/KICx45}$, and $Cx40^{KICx45/KICx45}$ mice, respectively. Total epicardial activation times deduced from these maps were 5, 7, and 10 ms, respectively. In the maps shown in B the sites of first activation were basolateral and apicolateral sites for $Cx40^{+/+}$, and $Cx40^{+/KICx45}$ and $Cx40^{KICx45/KICx45}$ mice, respectively. In these examples, the total epicardial activation times were 5, 6.5, and 6 ms, respectively. C, Representative curves of AV nodal conduction for the 3 groups of mice investigated. Relationship between the activation times of the RV is plotted as a function of the coupling interval of the premature stimulus. Black curves were drawn from experimental data; red curves are the best fits of the experimental data to online Equation 1 (available in the online data supplement).

mice have indicated that the increase in the duration of the P wave was higher, ranging from 30% to 56%,[20,21] and was mainly due to a very significant reduction of the CV (30%) in the RA.[21] These results, and the present data are suggestive of a chamber-specific role of Cx40. This hypothesis is strengthened by the fact that in the human heart the expression level of Cx40 is higher in the RA than in the LA.[39] However, this differential expression remains to be demonstrated in the mouse heart.

No differences were found in the various parameters that characterize the AV conduction in the $Cx40^{+/+}$, $Cx40^{+/KICx45}$, and $Cx40^{KICx45/KICx45}$ mice, indicating that the AV node func-

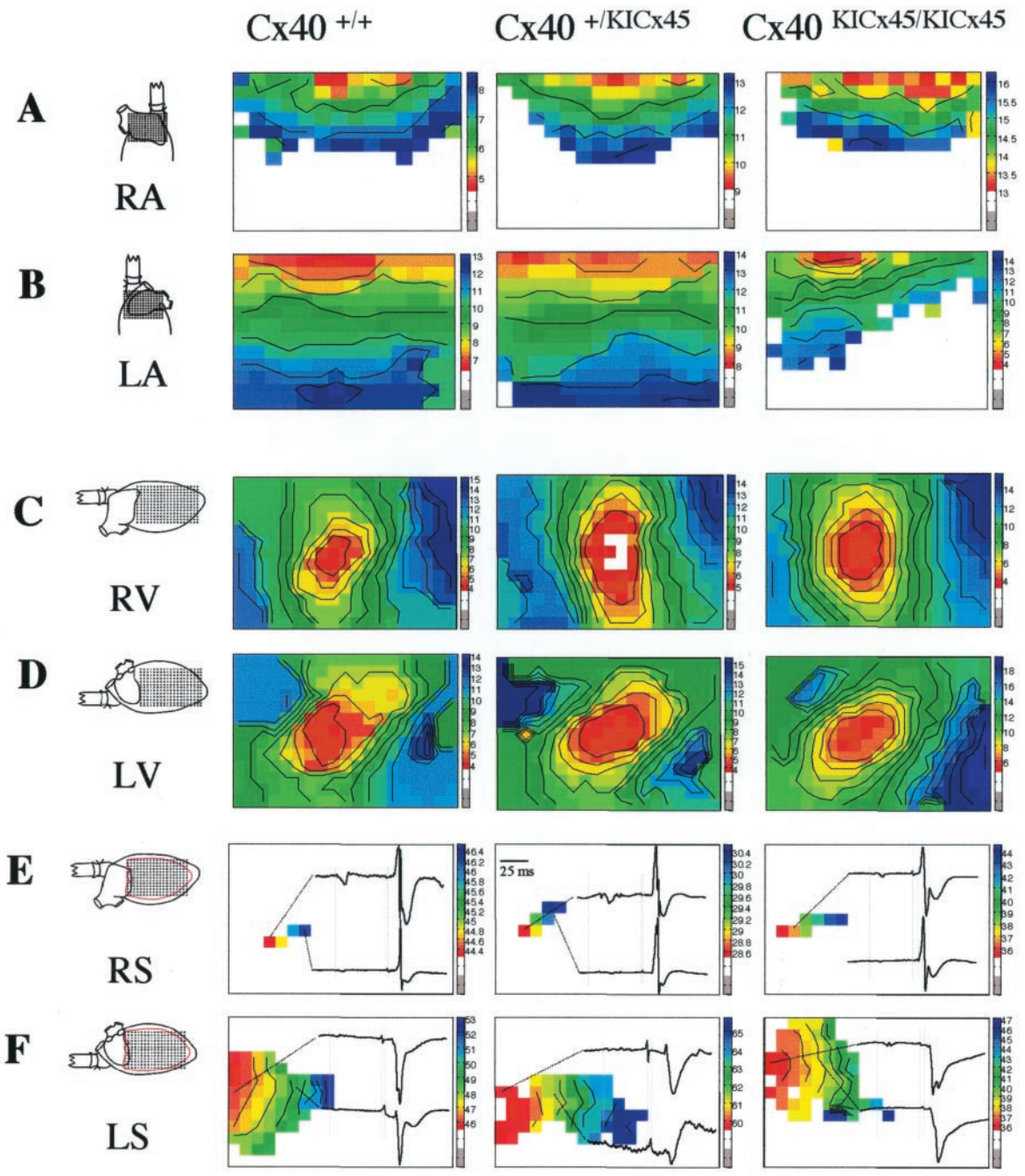


**Figure 6.** Representative paced activation maps of the RA and LA (A and B), the RV and LV (C and D), and the RBB and LBB (E and F) of $Cx40^{+/+}$, $Cx40^{+/KICx45}$, and $Cx40^{KICx45/KICx45}$ mice. Position of the electrode array on the epicardium (A through D) or the septal myocardium (E and F) is indicated in the pictograms. Activation times are relative to the pacing stimulus in the maps of the RA, LA, RV, and LV and relative to the atrial activation in the maps of the RBB and LBB. CVs were calculated from these maps. Activation times (ms) are indicated by color codes. In the examples shown in A and B, the CVs in the RA and the LA were 36 and 29, 32 and 32, and 41 and 19 cm/s for $Cx40^{+/+}$, $Cx40^{+/KICx45}$, and $Cx40^{KICx45/KICx45}$ mice, respectively. In the examples shown in C and D, the CVs in the RV and the LV were 40 and 38, 40 and 33, and 30 and 34 cm/s for $Cx40^{+/+}$, $Cx40^{+/KICx45}$, and $Cx40^{KICx45/KICx45}$ mice, respectively. Note that the anisotropy of the conduction in the ventricles is independent of the genotype. CVs determined from the activation maps of the RBB and LBB illustrated in E (RS, right side of the septum) and F (LS, left side of the septum) were 42 and 47, 54 and 51, and 17 and 54 cm/s for $Cx40^{+/+}$, $Cx40^{+/KICx45}$, and $Cx40^{KICx45/KICx45}$ mice, respectively. Note that the activation patterns in the right and left BB are asymmetrical. Electrograms recorded in 2 different sites of both bundle branches are shown for each genotype.

tions normally when Cx40 is replaced by Cx45. Numerous studies have described an increase in the PR interval and the Wenckebach cycle length in the Cx40 KO mice,[18–21] which indicated an impairment of the AV conduction. Our results indicate that the absence of Cx40 in the AV node can be corrected by the expression of Cx45 despite differences in their intrinsic properties.

The delayed activation of the RV, but not that of the LV, during SR, which increases the activation time of the heart, accounts for the increase of the duration of the QRS complex.

The CV in the ventricular working myocardium was unaffected by the replacement of Cx40 by Cx45, because Cx40 is not expressed in the ventricular working myocardium of the adult mouse heart. The slow CV measured in the RBB of $Cx40^{KICx45/KICx45}$ mice, but not in the LBB, explains the abnormal activation of the RV, in these animals. In the absence of Cx40, Cx45 is the only known Cx which is expressed in the proximal parts of the bundle branches.[5] Assuming that Cx45 was upregulated in a similar way in both bundle branches, its expression supports a normal conduction in the LBB, but fails to do so in the RBB, indicating that electrical and/or structural differences between LBB and RBB account for the observed effect. Analysis of mice in which one allele of the Cx40 gene was replaced by eGFP ($Cx40^{+/KIeGFP}$ mice) has shown that the LBB was in fact constituted with 20 or so parallel strands coming from the His bundle, and covering entirely the left side of the interventricular septum. In contrast, on the right flank the branch (RBB) emerging from the His bundle was constituted by only one thin fiber in its proximal part.[40] Thus, the LBB is more extended and much more complex than the RBB, and this morphology is in agreement with the activation patterns which were recorded (Figures 6E and 6F). Consequently, variations of the gap junctional coupling in the ventricular CS will affect RBB conduction more severely than LBB conduction. Furthermore, the relationship between the gap junctional coupling and the CV in a strand of model cells is not linear.[41] At high levels of junctional conductance the CV saturates, and significant reductions of the conductance from very high values do not necessarily result in a significant reduction of the CV. In contrast, small reductions of the conductance from low values will lead to drastic reductions of the CV. If one assumes that the coupling is higher in the LBB than in the RBB, which is not unlikely because the CV is higher in the LBB (47.8 cm/s) than in the RBB (36.5 cm/s), a similar reduction of the intercellular coupling in both bundle branches would be more prominent in the RBB than in the LBB. The analysis of Cx40KO mice confirmed that the RBB is much more sensitive to changes in the Cx expression than the LBB. Indeed, the deletion of Cx40 without replacement resulted in conduction block in the RBB, but induced only a slowing down of the conduction in the LBB.[25] The higher vulnerability of the RBB is also reflected in the clinical data that indicate that the frequency of conduction impairment in patients with cardiovascular diseases is much higher in the RBB than in the LBB (see for example Newby et al[42]).

In summary, the replacement of Cx40 by Cx45 resulted in the heart in a significant reduction of the CV in the LA and a normal CV in the RA. The conduction delay in the AV node was unaffected, whereas a partial loss of function became apparent in the RBB, but not in the LBB.

## Acknowledgments

This work was supported by the CNRS, the Université de la Méditerranée, the European Community (contract QLG1-1999-00516), The Netherlands Heart Foundation (grant 99-200), and the French Ministry of Education (ACI Biologie du Développement et Physiologie Intégrative). S.A. was supported (fellowships) by the Association Française contre les Myopathies, and the Groupe de Réflexion sur la Recherche Cardiovasculaire.

## References

1. Kanno S, Saffitz JE. The role of myocardial gap junctions in electrical conduction and arrhythmogenesis. *Cardiovasc Pathol*. 2001;10:169–177.
2. Harris AL. Emerging issues of connexin channels: biophysics fills the gap. *Q Rev Biophys*. 2001;34:325–472.
3. Evans WH, Martin PE. Gap junctions: structure and function. *Mol Membr Biol*. 2002;19:121–136.
4. Willecke K, Eiberger J, Degen J, Eckardt D, Romualdi A, Güldenagel M, Deutsch U, Söhl G. Structural and functional diversity of connexin genes in the mouse and human genome. *Biol Chem*. 2002;383:725–737.
5. Miquerol L, Dupays L, Théveniau-Ruissy M, Alcoléa S, Jarry-Guichard T, Abran P, Gros D. Gap junctional connexins in developing mouse cardiac conduction system. In: Goode J, ed. *Development of the Cardiac Conduction System* (Novartis Foundation, Symposium 250). Chichester, UK: Wiley; 2003:80–98.
6. Delorme B, Dahl E, Jarry-Guichard T, Marics I, Briand J-P, Willecke K, Gros D, Théveniau-Ruissy M. Developmental regulation of connexin 40 gene expression in mouse heart correlates with the differentiation of the conduction system. *Dev Dyn*. 1995;204:358–371.
7. Delorme B, Dahl E, Jarry-Guichard T, Briand J-P, Willecke K, Gros D, Théveniau-Ruissy M. Expression pattern of connexin gene products at the early developmental stages of the mouse cardiovascular system. *Circ Res*. 1997;81:423–437.
8. Coppen SR, Dupont E, Rothery S, Severs NJ. Connexin45 expression is preferentially associated with the ventricular conduction system in mouse and rat heart. *Circ Res*. 1998;82:232–243.
9. Coppen SR, Severs NJ, Gourdie RG. Connexin45 ($\alpha$6) expression delineates an extended conduction system in the embryonic and mature rodent heart. *Dev Genet*. 1999;24:82–90.
10. Verheijck EE, van Kempen MJ, Veereschild M, Lurvink J, Jongsma HJ, Bouman LN. Electrophysiological features of the mouse sinoatrial node in relation to connexin distribution. *Cardiovasc Res*. 2001;52:40–50.
11. Johnson CM, Kanter EM, Green KG, Laing JG, Betsuyaku T, Beyer EC, Steinberg TH, Saffitz JE, Yamada KA. Redistribution of connexin45 in gap junctions of connexin43-deficient hearts. *Cardiovasc Res*. 2002;53:921–935.
12. Alcoléa S, Théveniau-Ruissy M, Jarry-Guichard T, Marics I, Tzouanacou E, Chauvin JP, Briand JP, Moorman AF, Lamers WH, Gros DB. Down-regulation of connexin 45 gene products during mouse heart development. *Circ Res*. 1999;84:1365–1379.
13. Coppen SR, Kodama I, Boyett MR, Dobrzynski H, Takagishi Y, Honjo H, Yeh HI, Severs NJ. Connexin45, a major connexin of the rabbit sinoatrial node, is co-expressed with connexin43 in a restricted zone at the nodal-crista terminalis border. *J Histochem Cytochem*. 1999;47:907–918.
14. Verheule S, van Kempen MJ, Postma S, Rook MB, Jongsma HJ. Gap junctions in the rabbit sinoatrial node. *Am J Physiol*. 2001;280:H2103–H2115.
15. Krüger O, Plum A, Kim J-S, Winterhager E, Maxeiner S, Hallas G, Kirchhoff S, Traub O, Lamers WH, Willecke K. Defective vascular development in connexin 45-deficient mice. *Development*. 2000;127:4179–4193.
16. Kumaï M, Nishii K, Nakamura K, Takeda N, Suzuki M, Shibata Y. Loss of connexin45 causes a cushion defect in early cardiogenesis. *Development*. 2000;127:3501–3512.
17. Gutstein DE, Morley GE, Tamaddon H, Vaidya D, Schneider MD, Chen J, Chien KR, Stuhlmann H, Fishman GI. Conduction slowing and sudden arrhythmic death in mice with cardiac-restricted inactivation of connexin43. *Circ Res*. 2001;88:333–339.
18. Simon AM, Goodenough DA, Paul DL. Mice lacking connexin40 have cardiac conduction abnormalities characteristic of atrioventricular block and bundle branch block. *Curr Biol*. 1998;8:295–298.
19. Kirchhoff S, Nelles E, Hagendorff A, Krüger O, Traub O, Willecke K. Reduced cardiac conduction velocity and predisposition to arrhythmias in connexin40-deficient mice. *Curr Biol*. 1998;8:299–302.
20. Hagendorff A, Schumacher B, Kirchhoff S, Luderitz B, Willecke K. Conduction disturbances and increased atrial vulnerability in connexin40-deficient mice analyzed by transesophageal stimulation. *Circulation*. 1999;99:1508–1515.
21. Verheule S, van Batenburg CA, Coenjaerts FE, Kirchhoff S, Willecke K, Jongsma, HJ. Cardiac conduction abnormalities in mice lacking the gap junction protein connexin40. *J Cardiovasc Electrophysiol*. 1999;10:1380–1389.
22. Tamaddon HS, Vaidya D, Simon AM, Paul DL, Jalife J, Morley GE. High-resolution optical mapping of the right bundle branch in connexin40

knockout mice reveals slow conduction in the specialized conduction system. *Circ Res*. 2000;87:929–936.
23. VanderBrink BA, Sellitto C, Saba S, Link MS, Zhu W, Homoud MK, Estes NA III, Paul DL, Wang PJ. Connexin40-deficient mice exhibit atrioventricular nodal and infra-Hisian conduction abnormalities. *J Cardiovasc Electrophysiol*. 2000;11:1270–1276.
24. Bevilacqua LM, Simon AM, Maguire CT, Gehrmann J, Wakimoto H, Paul DL, Berul CI. A targeted disruption in connexin40 leads to distinct atrioventricular conduction defects. *J Interv Card Electrophysiol*. 2000; 4:459–467.
25. Van Rijen HVM, van Veen TA, van Kempen MJ, Wilms-Schopman FJ, Potse M, Krüeger O, Willecke K, Opthof T, Jongsma HJ, de Bakker JM. Impaired conduction in the bundle branches of mouse hearts lacking the gap junction protein connexin40. *Circulation*. 2001;103:1591–1598.
26. Gu H, Smith FC, Taffet SM, Delmar M. High incidence of cardiac malformations in connexin40-deficient mice. *Circ Res*. 2003;93:201–206.
27. Bukauskas FF, Elfgang C, Willecke K, Weingart R. Biophysical properties of gap junction channels formed by mouse connexin40 in induced pairs of transfected human HeLa cells. *Biophys J*. 1995;68:2289–2298.
28. Van Veen TA, van Rijen HVM, Jongsma HJ. Electrical conductance of mouse connexin45 gap junction channels is modulated by phosphorylation. *Cardiovasc Res*. 2000;46:496–510.
29. Beblo DA, Wang HZ, Beyer EC, Westphale EM, Veenstra RD. Unique conductance, gating, and selective permeability properties of gap junction channels formed by connexin40. *Circ Res*. 1995;77:813–822.
30. Moreno AP, Laing JG, Beyer EC, Spray DC. Properties of gap junction channels formed of connexin 45 endogenously expressed in human hepatoma (SKHep1) cells. *Am J Physiol*. 1995;268:C356–C365.
31. Hellmann P, Winterhager E, Spray DC. Properties of connexin40 gap junction channels endogenously expressed and exogenously overexpressed in human choriocarcinoma cell lines. *Pfügers Arch*. 1996;432: 501–509.
32. Barrio LC, Capel J, Jarillo JA, Castro C, Revilla A. Species-specific voltage-gating properties of connexin-45 junctions expressed in *Xenopus* oocytes. *Biophys J*. 1997;73:757–769.
33. Van Rijen HVM, van Veen TA, Hermans MM, Jongsma HJ. Human connexin40 gap junction channels are modulated by cAMP. *Cardiovasc Res*. 2000;45:941–951.
34. Van Veen TA, van Rijen HVM, Wiegerinck RF, Opthof T, Colbert MC, Clement S, de Bakker JMT, Jongsma HJ. Remodeling of gap junctions in mouse hearts hypertrophied by forced retinoic acid signaling. *J Mol Cell Cardiol*. 2002;34:1411–1423.
35. Wehrens XHT, Kirchhoff S, Doevendans PA. Mouse electrocardiography: an interval of thirty years. *Cardiovasc Res*. 2000;45:231–237.
36. Plum A, Hallas G, Magin T, Dombrowski F, Hagendorff A, Schumacher B, Wolpert C, Kim J-S, Lamers WH, Evert M, Meda P, Traub O, Willecke K. Unique and shared functions of different connexins in mice. *Current Biol*. 2000;10:1083–1091.
37. Kirchhoff S, Kim J-S, Hagendorff A, Thonnissen E, Krüger O, Lamers WH, Willecke K. Abnormal cardiac conduction and morphogenesis in connexin40 and connexin43 double-deficient mice. *Circ Res*. 2000;87: 399–405.
38. White TW. Unique and redundant connexin contribution to lens development. *Science*. 2002;295:319–320.
39. Vozzi C, Dupont E, Coppen SR, Yeh HI, Severs NJ. Chamber-related differences in connexin expression in the human heart. *J Mol Cell Cardiol*. 1999;31:991–1003.
40. Meysen S, Abran P, van Rijen HVM, Bois P, Gros P, Miquerol P. Analysis of the cardiac conduction system in transgenic mice knock-in Cx40eGFP. *Arch Mal Coeur Vaiss*. 2003;96:392. Abstract.
41. Jongsma HJ, Wilders R. Gap junctions in cardiovascular disease. *Circ Res*. 2000;86:1193–1197.
42. Newby KH, Pisano E, Krucoff MW, Green C, Natale A. Incidence and clinical relevance of the occurrence of bundle-branch block in patients treated with thrombolytic therapy. *Circulation*. 1996;94:2424–2428.